NUMERICAL MODEL FOR NON-DARCY FLOW THROUGH COARSE POROUS MEDIA USING THE MOVING PARTICLE SIMULATION METHOD

by

Tomoki IZUMI [a*] ***and Junya MIZUTA*** [b]

[a] Graduate School of Agriculture, Ehime University, Ehime, Japan
[b] Fukuyama City Office, Hiroshima, Japan

Original scientific paper
https://doi.org/10.2298/TSCI171231271I

A numerical model for non-Darcy flow, which occurs when water moves through coarse porous media under high Reynolds number, is developed. The governing equation for incompressible viscous flow through porous media is composed of a continuity equation and a momentum equation, which is the Navier-Stokes equation with an additional non-linear resistance term based on Forchheimer's law. For the discretization scheme, moving particle simulation method is employed. In order to assess the model validity, seepage experiments in different kinds of coarse porous media are implemented, and then reproducibility of the numerical results is examined. From the results, it is found that the computational flow velocities at middle part of porous media are in good agreement with experimental ones while velocities at outflow end are overestimated.

Key words: *non-Darcy flow, Forchheimer's law, particle method, numerical simulation, seepage experiment, coarse porous media*

Introduction

It is important to properly manage groundwater resources for sustainable water use in small rainfall area where water supply depends on groundwater at a large rate. Although groundwater flow or water movement through porous media is generally described by Darcy's law, it has been indicated that flow under high Reynolds numbers does not always satisfy the law [1]. This flow is known as non-Darcy flow, and it occurs in groundwater flow through coarse gravel riverbeds [2] and in pipe flow on heterogeneous mountain slopes [3]. Among them, studies on groundwater flow through coarse gravel riverbeds in fluvial fan area are useful for sustainable groundwater use since it can be considered that groundwater is recharged through interaction between river water and groundwater. Thus, it is important to develop a numerical model for non-Darcy flow in order to analyze groundwater flow and/or to estimate groundwater recharge because field observations of groundwater are relatively difficult compared with those of surface water such as river water.

Forchheimer equation and Izbash equation have been proposed as motion equation for non-Darcy flow, and the model parameters included in the equations have also been discussed. For example, Sidiropoulou *et al*. [4] compared and evaluated expressions of Forchheimer coefficients based on theoretical approaches and experimental analysis. Soni *et al*. [5] determined Izbash coefficients based on experimental results and discussed the factors influ-

* Corresponding author; e-mail: t_izumi@agr.ehime-u.ac.jp

encing the coefficients. Studies on numerical model for non-Darcy flow are found in the field of coastal engineering. Huang *et al*. [6] proposed a 2-D numerical model to simulate the interaction between a solitary wave and submerged porous breakwater. Shao [7] presented an incompressible smoothed particle hydrodynamics (ISPH) flow model to simulate wave interactions with a porous medium. Akbari and Namin [8] presented an ISPH flow model which can solve two porous and pure fluid flows simultaneously to simulate wave interaction with porous structures. Akbari [9] introduced modified moving particle method in porous media (MMPP) for simulating a flow interaction with porous structures. In the field of thermal science, Hamdan [10] performed a numerical investigation on the flow and convective heat transfer characteristics for isothermal parallel plate channel filled with porous media using the finite difference method. Motsa and Animasaun [11] developed a spectral collocation method to solve a problem of unsteady heat and mass transfer past a semi-infinite vertical plate with diffusion-thermo and thermophoresis effects in the presence of suction. Sayehvand *et al*. [12] numerically investigated forced convection heat transfer from two tandem circular cylinders embedded in a porous medium using the finite volume method. In their works, Forchheimer equation is used as motion equation. Studies on numerical model for non-Darcy flow cannot be found in the field of groundwater engineering.

In this study, a numerical model for non-Darcy flow is thus proposed as a powerful tool for sustainable groundwater use in the area where water supply depends on groundwater at a large rate. According to previous studies, the governing equation is composed of a continuity equation and a momentum equation, which is the Navier-Stokes equation to which a non-linear resistance based on Forchheimer's law instead of Darcy's law is added. For the discretization, however, moving particle simulation (MPS) method [13], one of the Lagrangian particle approach, is employed instead of the Eulerian grid approach such as the finite difference and finite volume method. This is because discretization of convective derivative term, which occurs undesirous numerical oscillation, is not required originally. MPS method was originally proposed by Koshizuka *et al*. [14] and was composed of particle interaction models localized by using a weight function. Koshizuka *et al*. [14] investigated the accuracy of MPS method in test calculations; a parabolic profile of the flow velocity was obtained in a Poiseuille flow. However, numerical stability of the incompressibility model was sensitive to a correction parameter used in the method. Therefore, Koshizuka and Oka [13] modified MPS method of [14] in terms of the weight function and modelling of incompressibility. ISPH method [15] is also one of the Lagrangian particle approach. The difference between MPS and ISPH method is found in weight function (or kernel). While ISPH method requires differentiability for the weight function, MPS method does not. Thus, MPS method is easy to handle for modelling. In order to assess the model validity, since the numerical accuracy of MPS method was shown as mentioned above, seepage experiments in different kinds of coarse porous media are implemented, and then reproducibility of the numerical results for the experimental results is examined.

Numerical model for non-Darcy flow

Numerical model for non-Darcy flow proposed in this study, governing equation, discretization method computation algorithm, and boundary conditions are explained.

Governing equation

The governing equation for incompressible viscous flow through porous media is composed of a continuity equation and a momentum equation, which is the Navier-Stokes equation to which a non-linear resistance based on Forchheimer's law is added:

$$\frac{\partial \rho}{\partial t} = 0 \tag{1}$$

$$\frac{C_\mathrm{r}}{n_\mathrm{w}} \frac{D\vec{u}}{Dt} = -\frac{1}{\rho_\mathrm{w}} \nabla p + \nu_\mathrm{E} \nabla^2 \vec{u} - a\vec{u} - bg\vec{u} \mid \vec{u} \mid + \vec{g} \tag{2}$$

with

$$C_\mathrm{r} = 1 + \frac{1 - n_\mathrm{w}}{n_\mathrm{w}} \gamma \tag{3}$$

$$\nu_\mathrm{E} = \frac{\nu_\mathrm{w}}{n_\mathrm{w}} \tag{4}$$

where $\vec{u}$ is the mean velocity vector, C_r – the inertia coefficient, n_w – the porosity, t – the time, ρ_w – the water density, p – the pressure, ν_E – the effective kinematic viscosity, a and b are the coefficients of Forchheimer's law, respectively, $\vec{g} = \{0, 0, g\}^\mathrm{T}$ – the gravitational acceleration vector, γ – a non-dimensional coefficient which accounts for the extra amount of momentum that is needed to accelerate the same volume of water in a porous medium [16], and ν_w – the kinematic viscosity. The first term on the right hand side of eq. (2) denotes the pressure force caused by the pressure gradient, the second term denotes the viscous force, the third and fourth terms denote the resistance force by the porous media, and the last term denotes the gravitational force. Since eq. (2) corresponds to the momentum equation based on the Darcy's law when the coefficient of $b = 0$, the coefficient a is described as $1/k_\mathrm{s}$ where k_s is the hydraulic conductivity. The coefficient b is dealt with a fitting parameter in this study because it depends on the properties of the porous medium only.

Discretization method

The MPS method [13] is used for the discretization scheme in this study. This method discretizes differential operators such as gradients or the Laplacian, based on the interaction model between particles within an interaction area determined by effective radius r_e, fig. 1. In the interaction model, the gradient and Laplacian models are defined:

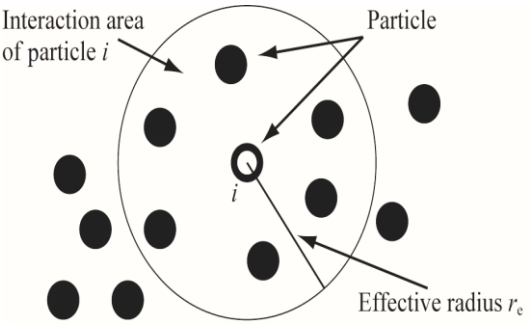

Figure 1. Effective radius and interaction area in the interaction model

$$\left\langle \nabla \phi \right\rangle_i = \frac{D_0}{n_0} \sum_{j \neq i} \left[\frac{\phi_j - \phi_i}{\left| \vec{r}_j - \vec{r}_i \right|^2} (\vec{r}_j - \vec{r}_i) \mathrm{w}(\mid \vec{r}_j - \vec{r}_i \mid) \right] \tag{5}$$

$$\left\langle \nabla^2 \phi \right\rangle_i = \frac{2D_0}{n_0 \lambda} \sum_{j \neq i} \left[(\phi_j - \phi_i) \mathrm{w}(\mid \vec{r}_j - \vec{r}_i \mid) \right] \tag{6}$$

where ϕ is a scalar variable, D_0 is the number of space dimensions, n_0 – the particle number density (which should be kept constant to satisfy the incompressible condition), $\vec{r}$ – the position vector, w(r) – the weight function (which describes the weight of interaction between two particles separated by distance r), λ – the model parameter, and i and j are particle numbers, respectively. The weight function, model parameter λ, and the particle number density are defined:

$$w(r)=\begin{cases}\frac{r_e}{r}-1 & (r\le r_e)\\ 0 & (r>r_e)\end{cases} \tag{7}$$

$$\lambda=\frac{\sum_{j\neq i}|\vec{r}_j-\vec{r}_i|^2\ w(|\vec{r}_j-\vec{r}_i|)}{\sum_{j\neq i}w(|\vec{r}_j-\vec{r}_i|)} \tag{8}$$

$$\langle n\rangle_i=\sum_{j\neq i}w(|\vec{r}_j-\vec{r}_i|) \tag{9}$$

Computation algorithm

A semi-implicit time marching scheme is used for the computation. Figure 2 shows the computation algorithm. In each time step k, the diffusion and source terms are explicitly calculated, and then the temporal velocities $\vec{u}^*$ and temporal positions $\vec{r}^*$ are obtained:

$$\vec{u}^*=\vec{u}^k+\frac{n_w\Delta t}{C_r}(\nu_E\nabla^2\vec{u}^k-ag\vec{u}^k-bg\vec{u}^k|\vec{u}^k|+\vec{g}) \tag{10}$$

$$\vec{r}^*=\vec{r}^k+\vec{u}^*\Delta t \tag{11}$$

Next, the Poisson equation for pressure (described below) is iteratively solved using the incomplete Cholesky conjugate gradient (ICCG) method, after which the time pressure values p^{k+1} are obtained:

$$\nabla^2 p^{k+1}=-\frac{C_r}{n_w}\frac{\rho_w}{(\Delta t)^2}\left(\frac{n^*-n^0}{n^0}\right) \tag{12}$$

Finally, the next time velocities $\vec{u}^{k+1}$ and positions $\vec{r}^{k+1}$ are obtained, after the temporal values have been corrected according to the pressure gradient.

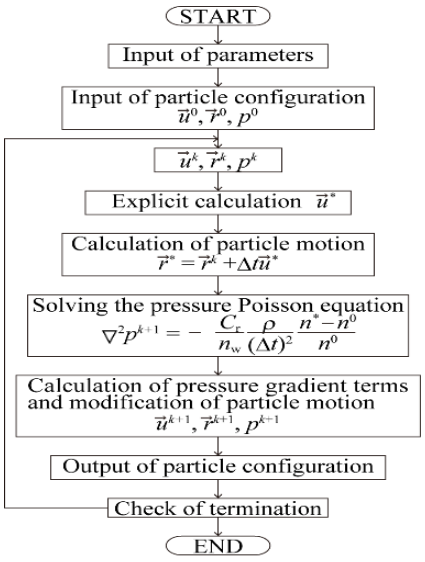

Figure 2. Computation algorithm

Boundary conditions

A free surface boundary is determined based on particle number density. When the particle number density satisfies:

$$\langle n\rangle_i<\beta n^0 \tag{13}$$

each particle is regarded as a free surface, where β is a parameter below 1.0. Under the condition, pressure is set to zero in the pressure calculation.

A wall boundary is represented as fixed particles. According to r_e, more than three layers of fixed particles are used to represent the wall in order to calculate the particle density number accurately. Velocity is set at zero for all fixed particles. Pressures are calculated only at the fixed particles in the innermost layer. The fixed particles in the other layers are only required to keep the particle number density around n^0 without calculating pressure.

An inflow boundary is represented as moving particles. Velocities and pressures are given to the particles at the boundary.

Validation

Validity of the numerical model proposed in this study is investigated in terms of the reproducibility for experimental results since the numerical accuracy of MPS method was shown in the previous studies. In this section, seepage experiments using different kinds of porous media are firstly explained, conditions of simulation by MPS method are then described, and computation results are finally discussed.

Table 1. Physical properties of porous media

	Gravel 1	Gravel 2	Glass beads
Porosity	0.46	0.46	0.40
Mean particle diameter [m]	$1.5\cdot10^{-2}$	$8.0\cdot10^{-3}$	$5.0\cdot10^{-3}$
Hydraulic conductivity [ms^{-1}]	$2.7\cdot10^{-2}$	$2.7\cdot10^{-2}$	$1.5\cdot10^{-2}$

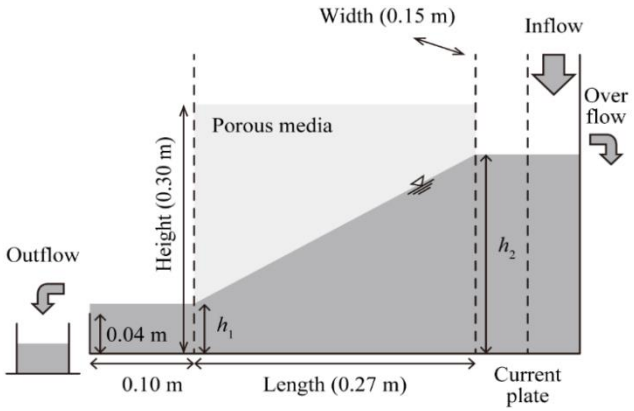

Figure 3. Schematic of the experiment

Experiment of flow through porous media

Seepage experiments using three kinds of porous media are implemented. Physical properties of the media are obtained by laboratory tests and summarized in tab. 1. The porosity, mean particle diameter, and hydraulic conductivity for the porous media are measured by water evaporation method, sieve analysis, and constant head permeability test, respectively. The schematic of the experiment is shown in fig. 3. Each porous medium is set at the size of 0.30 × 0.27 × 0.15 m (height × length × width). Water is poured into the right hand side of soil layer to keep water depth h_2 constant. Then outflow from the left hand side of soil layer and water depth at the inflow and outflow ends (h_1 and h_2) are measured. For each porous medium, at most six kinds of hydraulic gradient are set.

Simulation conditions

Numerical simulations of 2-D seepage flow in the cases corresponding to the seepage experiments mentioned above are implemented. Figure 4 shows an example of the initial state of the simulation domain for the MPS method, using computational particles with 0.01 m in diameter. The right hand side is set as the inflow boundary and the inflow particles are generated to keep water depth h_2 constant. The simulations are continued until achieving steady-state with time step of $1.0\cdot10^{-3}$ seconds. Parameters used in the simulations are summarized in tab. 2.

Results and discussion

Figures 5-7 show the relations between the velocity with hydraulic gradient in order to compare computational with experimental flow velocity at the middle part and outflow end in each porous medium. Figures 5-7 also show the plots based on Darcy's law in terms of experimental flow velocity at the outflow end, which are specified as u_D. The relation representing linearity such as u_D means that flow can be regarded as Darcy flow, and the relation re-

presenting non-linearity, on the other hand, means that flow can be regarded as non-Darcy flow. Also, the plots of experimental flow velocity have the error bar of 20% for the experimental data. Additionally, tab. 3 shows the errors between computational and experimental flow velocity at the middle part and outflow end in each porous medium. Note that superscript "o" and "m" denote *outflow* and *middle*, respectively. The coefficients *b* in gravel 1, gravel 2, and glass beads which are to be fitting parameters in this study are 60 m^{-1}, 60 m^{-1}, and 110 m^{-1}, respectively.

From figs. 5-7, it can be seen that all relations between the experimental flow velocity and hydraulic gradient are nonlinear and thus flows through porous media are non-Darcy flow. It is also found that the computational flow velocities at the middle part agree with experimental ones. Except for the plots at higher hydraulic gradient, computational flow velocities are plotted within 20% of experimental ones. From tab. 3, errors are in the range of 0.0008-0.0131 m/s. However, all of the computational flow velocities at the outflow end are overestimated. Errors are in the range of 0.0268-0.0731 m/s and it seems that errors become large as porosity and/or mean particle diameter increase.

To investigate the discrepancy in velocity, the coefficients in Forchheimer's law are discussed. Since the coefficient *b* is dealt with a fitting parameter in computation, the coeffi- cient *a* is focused on. Table 4 shows the coefficients of computations and experiments. In computation, *a* is defined as a reciprocal number of hydraulic conductivity. The coefficients of experiment are obtained from the fitting curve for experimental results shown in figs. 5-7. From tab. 4, it is found that values in computation are approximately ten times larger than those in experiment. Thus it is considered that modelling of coefficient *a* influences on the accuracy of computational re-

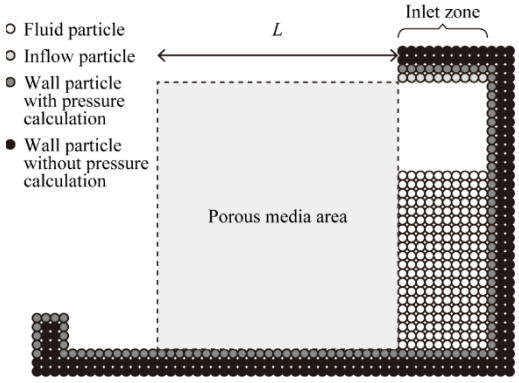

Figure 4. Initial state of the simulation domain for the MPS method

Table 2. Parameters used in the simulations

	Unit	Value
Kinematic viscosity (ν_w)	m^2s^{-1}	$1.0 \cdot 10^{-6}$
Density of water particles (ρ_w)	kgm^{-3}	1,000
Particle diameter (l_0)	m	0.01
Effective radius (r_e)	m	2.1 l_0
γ	–	0.34
β	–	0.97

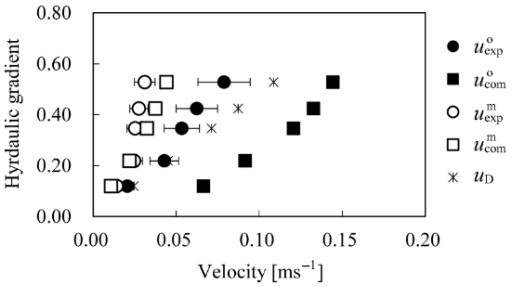

Figure 5. Comparison of computational with experimental velocity in gravel 1

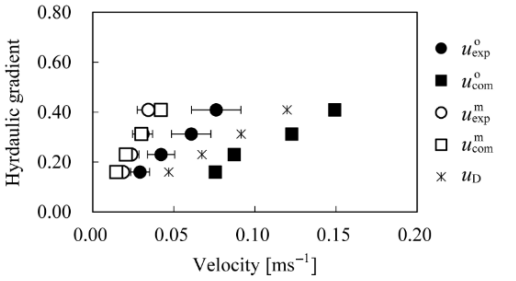

Figure 6. Comparison of computational with experimental velocity in gravel 2

sults. There are some previous studies on determination of the coefficients *a* and *b* in Forchheimer's law, *e. g*. [4]. Therefore it is necessary to exam the previous models for the coefficients *a* and *b* in Forchheimer's law and to revise description of *a* and *b* in order to improve the reproducibility of the numerical model developed.

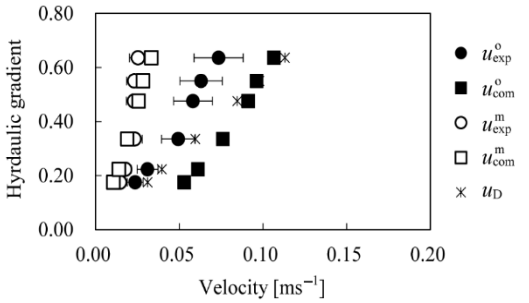

Figure 7. Comparison of computational with experimental velocity in glass beads

Conclusion

A numerical model for non-Darcy flow through coarse porous media is developed. The governing equation is a continuity equation and momentum equation which is Navier-Stokes equation to which a non-linear resistance based on Forchheimer's law instead of Darcy's law is added. MPS method is used for the discretization scheme. In order to examine the model validity, seepage experiments for three kinds of porous media are implemented. From the comparison of computational and experimental results, it is found that the computational flow velocities at middle part of porous media are in good agreement with experimental ones while velocities at outflow end are overestimated. Improvement of the reproducibility of the numerical model should be investigated for future task.

Table 3. Errors between computational and experimental flow velocity (= $u_{com} - u_{exp}$)* at the middle and outflow end

Hydraulic gradient	(1)		(2)		(3)		(4)		(5)		(6)	
	Outflow end	Middle	Outflow end	Middle	Outflow end	Middle	Outflow end	Middle	Outflow end	Middle	Outflow end	Middle
Gravel 1	0.0459	−0.0034	0.0488	−0.0028	0.0673	0.0071	0.0703	0.0099	0.0656	0.0131	–	–
Gravel 2	0.0464	−0.0042	0.0451	−0.0034	0.0620	−0.0008	0.0731	0.0077	–	–	–	–
Glass beads	0.0293	−0.0039	0.0301	−0.0038	0.0268	−0.0043	0.0330	0.0027	0.0332	0.0052	0.0332	0.0080

* in [ms^{-1}]

Table 4. Comparison of coefficient *a* in Forchheimer's law

	a	
	Computation	Experiment
Gravel 1	37.0	4.86
Gravel 2	37.0	3.41
Glass beads	66.7	5.62

Acknowledgment

This study is supported by JSPS 17K15346.

Nomenclature

- a – coefficient of linear term in Forchheimer's law, [sm^{-1}]
- b – coefficient of non-linear term in Forchheimer's law, [s^{2}m^{-2}]
- C_r – inertia coefficient, [–]
- D_0 – number of space dimension, [–]
- d_{50} – mean particle size, [m]
- g – gravitational acceleration, [ms^{-2}]
- $\vec{g}$ – gravitational acceleration vector, [ms^{-2}]
- h_1 – water depth at an outflow end of porous media, [m]
- h_2 – water depth at an inflow end of porous media, [m]
- k_s – hydraulic conductivity, [ms^{-1}]
- n^0 – particle number density to be kept constant, [–]

n_0 – particle number density, [–]
n_w – porosity, [–]
p – pressure, [Nm^{-2}]
$\vec{r}$ – position vector, [m]
r – distance between two particles ($=|\vec{r}_j - \vec{r}_i|$), [m]
r_e – effective radius, [m]
t – time, [s]
$\vec{u}$ – mean velocity vector, [ms^{-1}]
w() – weight function

Greek symbols

β – parameter used when determining a free surface, [–]
γ – coefficient which accounts for the extra amount of momentum, [–]
λ – relaxation coefficient in Laplacian model of MPS model, [–]
ν_E – effective kinematic viscosity, [m^2s^{-1}]
ν_w – kinematic viscosity of water, [m^2s^{-1}]
ρ_w – water density, [kgm^{-3}]
ϕ – scalar variable

Superscript

k – time step

Subscripts

i, j – particle number
exp – experimental
com – computational

References

[1] Bear, J., *Dynamics of Fluids in Porous Media*, American Elsevier Publishing Company, Inc., Cambridge, Massachusetts, USA, 1972
[2] Yamada, H., *et al*., Measuring Hydraulic Permeability in a Streamed Using the Packer Test , *Hydrological Processes*, *19* (2005), 13, pp. 2507-2524
[3] Kitahara, H., Characteristics of Pipe Flow in a Sub-surface Soil Layer on a Gentle Slope (II): Hydraulic Properties of Pipes (in Japanese), *Journal of the Japanese Forest Society*, *71* (1989), 8, pp. 317-322
[4] Sidiropoulou, M. G., *et al*., Determination of Forchheimer Equation Coefficients *a* and *b*, *Hydrological Processes*, *21* (2007), 4, pp. 534-554
[5] Soni, J. P., *et al*., An Experimental Evaluation of non-Darcian Flow in Porous Media, *Journal of Hydrology*, *38* (1978), 3-4, pp. 231-241
[6] Huang, C.-J., *et al*., Structural Permeability Effects on the Interaction of a Solitary Wave and a Submerged Breakwater, *Coastal Engineering*, *49* (2003), 1-2, pp. 1-24
[7] Shao, S., Incompressible SPH Flow Model for Wave Interactions with Porous Media, *Coastal Engineering*, *57* (2010), 3, pp. 304-316
[8] Akbai, H., Namin, M. M., Moving Particle Method for Modeling Wave Interaction with Porous Structures, *Coastal Engineering*, *74* (2013), Apr., pp. 59-73
[9] Akbari, H., Modified Moving Particle Method for Modeling Wave Interaction with Multi Layered Porous Structures, *Coastal Engineering*, *89* (2014), July, pp. 1-19
[10] Hamdan, M. O., An Empirical Correlation for Isothermal Parallel Plate Channel Completely Filled with Porous Media, *Thermal Science*, *17* (2013), 4, pp. 1061-1070
[11] Motsa, S. S., Animasaun, I. L., A New Numerical Investigation of Some Thermos-Physical Properties on Unsteady MHD non-Darcian Flow Past an Impulsively Started Vertical Surface, *Thermal Science*, *19* (2015), 1, pp. S429-S258
[12] Sayehvand, H.-O., *et al*., Numerical Analysis of Forced Convection Heat Transfer from Two Tandem Circular Cylinders Embedded in a Porous Medium, *Thermal Science*, *21* (2017), 5, pp. 2117-2128
[13] Koshizuka, S., Oka, Y., Moving-Particle Semi-implicit Method for Fragmentation of Incompressible Fluid, *Nuclear Science and Engineering*, *123* (1996), 3, pp. 421-434
[14] Koshizuka, S., *et al*., A Particle Method for Incompressible Viscous Flow with Fragmentation, *Computational Fluid Dynamics J.*, *4* (1995), 1, pp. 29-46
[15] Shao, S., Lo, E. Y. M., Incompressible SPH Method for Simulating Newtonian and non-Newtonian Flows with a Free Surface, *Advances in Water Resources*, *26* (2003), 7, pp. 787-800
[16] van Gent, M. R. A., Porous Flow Through Rubble-mound Material, *Journal of Waterway, Port, Coastal, and Ocean Engineering*, *121* (1995), 3, pp. 176-181

Paper submitted: December 31, 2017
Paper revised: March 28, 2018
Paper accepted: March 28, 2018